Anaerobic Wastewater Treatment

Ge Gao, Maithili Gokarn, Walker Grimshaw, Caitlin Rose McKinley, Liankun Zhu

December 14, 2013

Abstract

Wastewater treatment is an important issue worldwide. As AguaClara has grown, it has become increasingly important to not only improve methods for the treatment of drinking water, but also to treat community wastewater in a sustainable manner. The long term goals of this research are to develop a gravity driven system for wastewater treatment and to characterize the general mechanism for anaerobic waste treatment. This team will operate under the principles of reducing human impact on the environment by effectively treating domestic wastewater before reintroduction to natural bodies of water and treating waste as a source of energy rather than a sink.

Introduction

Wastewater treatment is the process of treating the sewage water from municipal sources before the wastewater isreintroduced to the environment. In a typical wastewater treatment process, solid contaminants are removed from the liquid stream, and the water is treated for chemical and biological contaminants. Treatment plants result in at least two effluent streams, treated water ready to flow back into the environment and treated biosolids suitable for reuse (e.g. fertilizer). In addition to the water being treated, the differences in wastewater treatment and drinking water treatment processes have to do with the additional necessity of sludge treatment. The standards of the effluent water between the two processes are necessarily held at different standards. Understandably, wastewater has much more matter in its stream that needs to be treated. Drinking water treatment processes treat an influent stream of raw water from rivers, lakes, or groundwater sources. Wastewater treatment processes often contain a unit operation for the digestion of organic matter, i.e. breaking down solid organic biomass using microbes and converting it into biogas, typically carbon dioxide and methane [12]. The AguaClara wastewater treatment division plans to use anaerobic digestion, microbial decomposition of organic matter in the absence of oxygen, in its treatment process.

Wastewater treatment is a necessary and beneficial process for all communities, regardless of socio-economic status. Wastewater from homes in under-

developed areas of the world is often left untreated before reintroduction to natural water sources, at a rate of about 2 million tons of waste per day [16]. This lack of treatment diminishes the already short supply of clean fresh water and increases the demand for more water treatment. With the addition of a wastewater system, water gets treated for contaminants before it reenters the environment. The risks of waterborne diseases like typhoid or cholera are lessened for people who collect raw water from public water sources for personal consumption [14].

The benefits of wastewater treatment can be seen through the utilization of biogas. Methane produced as a byproduct of anaerobic digestion can be utilized as a source of energy for powering the building, heating the digester, or driving machinery if enough biogas is harvested [15].

AguaClara has a strong background in creating sustainable, energy-efficient, and cost-efficient drinking water treatment technologies in developing nations. One of its newest challenges is developing the same level of efficiency for wastewater treatment technology. The AguaClara Wastewater Division, newly established in early 2013, aims to adapt the drinking water treatment innovations to the wastewater environment. The division's first project is the development of an anaerobic digestion bioreactor. The team wishes to expand upon research conducted over summer 2013 in finding ideal reactor specifications to maximize the rate and extent of anaerobic digestion. Additionally, the team seeks to discover methods of maximizing methane production and capture and minimizing oxygen levels in the system.

Literature Review

1 Energy Potential in Wastewater Treatment

Currently , in places where water is in limited supply ,the process of recovering valuable energy and materials from wastewater during treatment and/or using the final wastewater for non-drinking purposes (e.g agriculture) is widely practiced.There are three energy forms that are mainly used from the wastewater. Firstly, nitrogen and phosphorus from wastewater can be used for fertilizer instead of manufactured fertilizers. Secondly, potential energy might be gained from the thermal heat contained in water. Thirdly, the most commonly exploited energy source is the chemical energy that is contained in wastewater organics [2].

With conventional approaches involving aerobic treatment, a quarter to half of a plants' energy needs might be satisfied by using the methane (CH_4) fraction of the biogas produced from organic compounds during anaerobic digestion. Other plant modifications might further reduce energy needs considerably. If more of the wastewaters' potential energy were captured or energy inputs is reduced, then wastewater treatment may become a net energy producer. According to McCarty et. al., complete anaerobic treatment has the potential

Table 1: Typical Chemical Composition of Biogas from Wastewater Treatment [13]

Gaseous Component	Percentage by Volume
Methane (CH4)	60-75%
Carbon Dioxide (CO2)	19-33%
Nitrogen (N2)	1%
Oxygen (O2)	<0.5%
Water (H2O)	6%

to achieve net energy production while meeting stringent effluent standards [3]. Apart from the potential energy, the CH_4 is also a powerful greenhouse gas with a global warming potential about 25 times that of CO_2[3] and thus cannot be allowed to escape to the atmosphere but should be collected and reused.Table 1 provides the chemical composition of biogas from wastewater treatment processes.

2 Different Technologies within Anaerobic Wastewater Treatment

Knowing the various advantages that anaerobic wastewater treatment has over aerobic wastewater treatment, considerable effort has been put into developing different types of reactors in order to optimize the use of this technology. Each type of reactor has its unique feature which eventually serves to reach the common goal of producing clean water and increasing efficiency by using the methane gas produced in the process to run the reactor.

UASB - Upflow Anaerobic Sludge Blanket

Within the anaerobic treatment sphere, Upflow Anaerobic Sludge Bed (UASB) reactors are some of the most compact in design and have the ability to treat the highest loading rates. These have been selected for initial investigation and adaptation for effective implementation in developing nations. Aiyuk, et al. review the structure and operation of a UASB, the competing biocatalyzed reactions that occur in the reactor, and the challenges that come up during operation, such as ensuring sludge granulation during start-up and inhibiting disintegration over time [4]. The UASB reactor initially inoculated with sludge, often in granular form though it may be in a flocculent form, and operated with liquid flowing upward from the bottom of the reactor. The upflow operation of the system causes the wastewater to flow by the dense sludge in the bottom of the reactor and fluidize the less dense sludge blanket above.The microbes within the inoculum grow throughout the life of the reactor and may evolve sludge of varying qualities; flocculent inoculum may even form granules by itself. Sludge evolution is believed to depend on the Organic Loading Rate (OLR) and Sludge

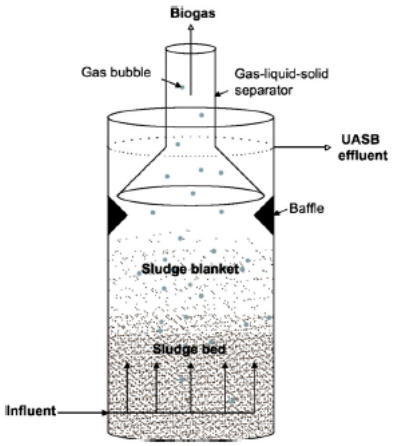

Figure 1: A standard reactor design, including the inverted funnel to serve as the GLS separator at the top of the reactor [6].

Loading Rate (SLR) during startup, though it has been shown the presence of bivalent and multivalent cations such as Ca^{+2} may also play an important role in granule formation [6], [5]. Granules ideally prevent the need for support materials in UASBs, though the plan is to investigate the effect of support materials in granule formation.

In a well operating reactor, gas is produced, containing primarily methane and carbon dioxide. The gas serves to further fluidize the reactor, assists in mixing, and the methane within the biogas may serve as an energy source if effectively captured [6]. This depends greatly upon the design of the Gas/Liquid/Solid (GLS) separator, typically a funnel type design to capture as much gas as possible, allow liquids to flow out of the reactor, and direct solids downward to the body of the reactor. It is commonly believed the sharp angles of the GLS separator assist in the redirection of the solids so most full-scale UASBs operate with a GLS separator similar to that shown in figure 1. Since the chemical oxygen demand(COD) produced is converted to methane, it is important to check how this can be carried out efficiently. Here, the influent COD concentration, hydraulic retention time and temperature play an important role. The focus must be placed on the conversion of COD to biogas and not only on the COD removal to ensure stable performance of the reactor, because the removal of COD varies with the hydraulic retention time and temperature[11].

If wastewater treatment has any chance of being a net energy producer, methane capture must be extremely effcient. Though COD removal rates and CH4 production rates are historically high for UASBs, Lobato et al. has demonstrated discrepancies between COD rates and CH4 rates, indicating methane losses within the system[7]. These losses are often unaccounted for, likely due to the absence of methane use for energy in many reactors, especially those constructed in the early days of the technology used for industrial wastewater

treatment[8]. The UASB reactor designs have changed and improved since the invention of the technology; however, post treatment is still widely believed to be necessary to meet effuent standards before discharge into the natural environment. Chong et al discuss many possible options. The technologies deemed most appropriate for exploration are constructed wetlands, downward hanging sponges, and pond systems[6]. These systems improve COD, nutrient, and pathogen removal, though other very different strategies have been proposed to improve independence of treatment effciency from ambient temperature as well as to increase nutrient removal. One simple strategy would be source separation of nutrients by urine diversion, though this would lead to a very different wastewater.

AFBR - Anaerobic Fluidized Bed Reactor

In the Anaerobic Fluidized Bed Reactor, the biofilm attaches itself to an inert media and grows around it. When liquid passes through these biogranules (biofilm plus carrier inert material), the bed of bio granules expands and is suspended in the liquid creating a fluidized state. The drag on the biogranules and their buoyancy must be great enough to balance the weight of the media to allow fluidization. Biofilm is more homogenous and smooth under conditions of high liquid velocity (high shear) than under low shear[9].Three kinds of models have have been developed based on the factors or elements that go in designing an AFBR.

The bed fluidization model by Nicolella et al., 2002 emphasizes the importance of the fluidization characteristics like terminal velocity and the size of the particles that allow efficient performance.[9] According to Fan et al, 1984, the fluidization of the bio granules occurs smoothly in a homogenous expansion i.e., when the particles are of uniform size. When the particles are not uniform, then there is a high tendency that segregation of particles will occur because of heterogeneous expansion. The other physical characteristics that contribute to using the right media is density, hardness, roughness of the media particles and the chemical characteristics are chemical adsorption and inertia[10]. Schreyer and Coughlin (1999) found that the disadvantage of this process is the possibility of an increase in thickness of the biofilm. This happens as the biofilm is continuously growing. Increase in thickness in biofilm results in decrease in the particle's overall density and increase in its buoyancy, which causes biofilm detachment from the media particle and subsequently gives rise to wash out problems [9].

Most anaerobic technologies still require some sort of additional polishing unit after the initial COD removal, and Kim et al used a two-stage system to evaluate the performance of an Anaerobic Fluidized Membrane Bioreactor (AFMBR). A 120-d continuous-feed evaluation was conducted using this two-stage anaerobic treatment system operated at 35 °C and fed a synthetic wastewater with

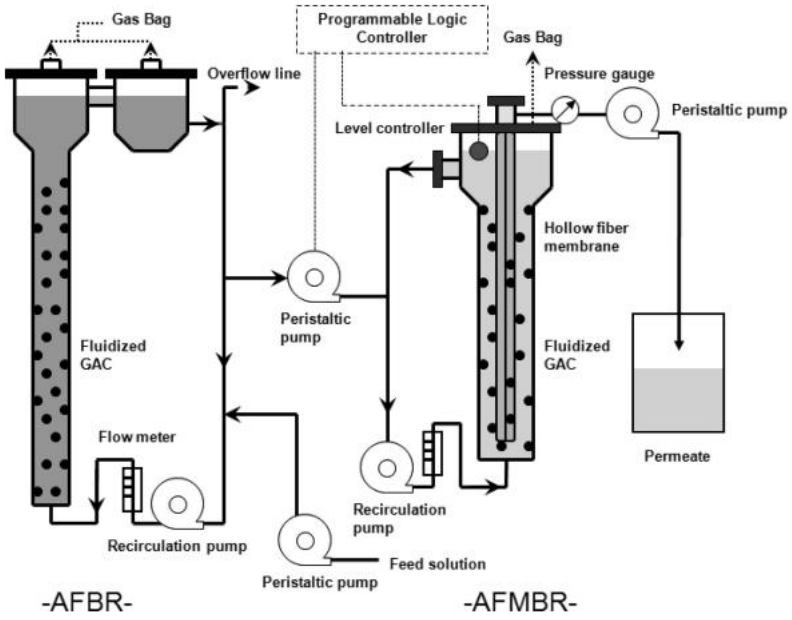

Figure 2: Diagram of AFBR and AFMBR combination setup. The AFMBR wasused in this study as a post treatment step after most of the COD was removed in the AFBR. These reactors use an expansion rather than contraction as part of the GLS separator to settle solids back into the main body of the reactor as well as a small settling tank after the AFBR[3].

chemical oxygen demand (COD) averaging 513 mg/L [3]. The first-stage was a similar fluidized-bed bioreactor without membranes (AFBR), operated at 2.0-2.8 h hydraulic retention time (HRT), and was followed by the above AFMBR, operating at 2.2 hr HRT [3]. The design of AFBR and AFMBR reactors are similar to UASB reactor designs, but some of the differences are shown in figure 2.

It was found that AFMBR requires 0.028KWh/m^3which is only a small fraction of the reported 0.25-1.0KWh/m^3 energy required in AFBR therefore the potential energy advantage of the AFMBR is apparent. And AFMBR can reduce the effluent TCOD of AFBR and thus increase the overall COD removal for the two-stage system to 99% [3]. AFMBR also can remove the effluent TSS and VSS of AFBR to near zero. In summary, the AFMBR used for post-treatment of effluent from an AFBR produced an excellent polished effluent.

Methods

COD

The influent and effluent water running through the reactor are tested for chemical oxygen demand daily. The water samples are stored in the freezer between sampling and the COD test to ensure the integrity of the COD samples. The COD is measured using prepackaged vials from CHEMetrics. The samples are left in the test vials for a two hour period, then the decrease in dichromate concentration is measured colorimetrically by the use of a Hewlett Packard Diode Array Spectrophotometer. By creating a standard curve from samples of known COD concentration, the concentration of the wastewater samples can be determined from the transmittance readings of the spectrophotometer.

Chemical oxygen demand is a way to measure the organic matter in a sample in terms of the amount of oxygen needed to fully oxidize the organic compounds. The most basic objective of wastewater treatment is to decrease the chemical oxygen demand to a low enough level to be introduced into the environment without causing negative effects such as hypoxia of water bodies.

Gas Chromatography

Gas chromatography with a Termal Conductivity Detector (TCD) is the chosen method to quantify the methane production in the reactor. Each day, a 100 μL sample of biogas is taken from the gas chamber. This sample is injected into the Hewlett Packard Gas Chromatograph and the chromatography is performed using a carrier gas of helium (He). The elution times and peak areas are recorded, and the peak areas are used to calculate the methane partial pressure through a standard curve procedure similar to that referenced in the COD method. The methane production is measured to determine the possible energy that could be produced by the reactor.

Gas chromatography has also been used to quantify the concentration of dissolved methane in the reactors. A standard curve for this analysis was created by injecting known amounts of pure methane into sealed 126 mL serum bottles already containing 90 mL water. The liquid and gas phases were allowed to equilibrate, then 5 mL of the liquid was removed from the serum bottle and injected into a smaller 9 mL sealed serum bottle, where again, the liquid and gas phases were allowed to equilibrate. A 0.5 mL sample of the headspace from the smaller bottle was then submitted to gas chomatography. The methane partial pressure of each sample was calculated using a Henry's constant of 1.4 mM/atm and the known volume of methane injected into the larger serum bottle [19]. For analysis purposes, a 5 mL sample was taken from a reactor near the effluent port and injected into a sealed 9 mL serum bottle, as during the creation of the standard curve.

State	Order	Time (s)
Tap Water, Stir Plate Off	1	20.5
Tap Water, Stir Plate On	2	35
Stock, Stir Plate On	3	4.5

Table 2: Sequence and time of each state within the Process Controller file to control pumping of stock into the reactors

Process Controller

The Process Controller file used for the operation of the reactor has three states that rotate only based upon time. These time steps control the tap water and stock valves to dilute the stock by a 18.5 : 1.5 ratio to achieve an influent COD of 500 mg/L. The states control the tap and stock valves as well as the stir plate to mix the concentrated stock solution within the refrigerator and are repeated during reactor operation. The sequence and time of the states for each reactor are shown in table 2.

The pressure within the gas chamber is recorded by a pressure sensor as indicated in Figure 3. As gas is produced and fills the chamber, the differential pressure between the two ports decreases. When the water level in the chamber reaches the setpoint of 2 cm above the lower port, the gas valve opens, releasing gas until the water level rises to the other setpoint of 7 cm above the lower port, at which point the gas valve closes and the chamber begins to once again collect gas. The pressure measured by the pressure sensor is recorded in a Microsoft Excel file every 30 seconds. This pressure data is then graphed and the number of off-gas events is visually determined in order to calculate the daily gas production within the reactor.

Synthetic Wastewater Preparation

The synthetic wastewater used in the experiments was modeled after the synthetic wastewater used by Aiyuk et al. [17]. The constituents of the wastewater and appropriate concentrations are shown in table 3. The synthetic wastewater is diluted by a factor of 12.3 when pumped into the reactor to achieve an influent COD of 500 mg/L. After preparation, the wastewater is sterlized in the autoclave before use. Normally prepared in a 5L container, the stock is autoclaved for 1 1/2 hours at 121^0C.

Bed Expansion

It has previously been stated that for a sand bed, double the minimum fluidization velocity causes the bed to expand approximately 30%. The team has conducted experiments in order to characterize the relationship between upflow velocity and bed expansion in order to more accurately control the size of the particle beds in the AFBR reactors.

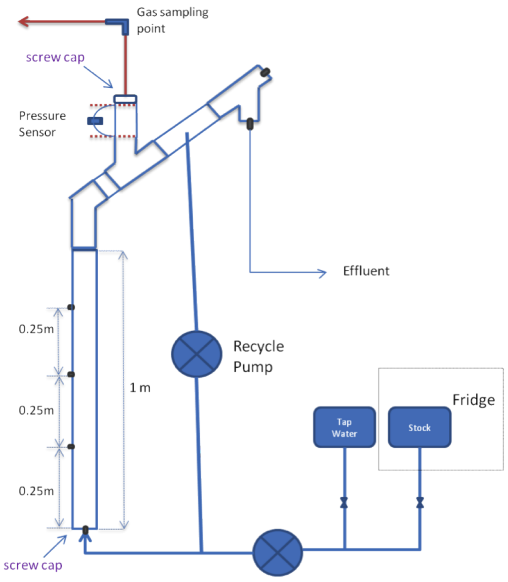

Figure 3: Diagram of Reactor Design. Stock is diluted with tap water as it flows from the refrigerator into the base of the reactor. The recycle pump is only used in the three AFBR reactors, but it is not used in the three UASB reactors. The gas chamber is capped with a removable screw cap to allow access to the body of the reactor for cleaning and unclogging. Gas is sampled through a septa at the gas sampling point and submitted to gas chromatography.

Chemical Constituent	Amount added (mg/L)
Urea	1600
NH_4	200
Na-Acetate	1357
Peptone	300
$MgHPO_4$-$3H_2O$	500
K_2HPO_4	305
$FeSO_4$-$7H_2O$	100
$CaCl_2$-$2H_2O$	120
Starch	2100
Milk Powder	2000
Yeast Extract	900
Vegetable Oil	500
$CuCl_2$-$2H_2O$	10
$MnSO_4$-H_2O	2
$NiSO_4$-$6H_2O$	5
$ZnCl_2$	5

Table 3: 12 1/3 x Concentrated Synthetic Wastewater Recipe [4]

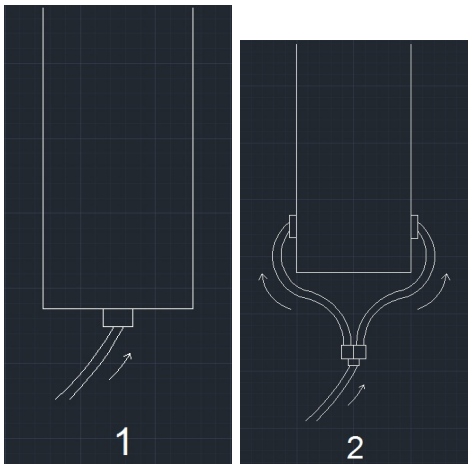

Figure 4: The two inlet geometries used for bed expansion testing.

In order to compensate for the delayed arrival of media , the group decided to use sand media of different sizes that was readily available. Upon sieving playground sand, four different grain sizes were differentiated, ranging from 0.84 mm to 0.07 mm in diameter, though only small only approximately 50 mL of each size sand could be obtained. The minimum fluidization velocity and corresponding reactor flow rate were calculated using equation 1 and the particle diameters obtained by sieving. The sand of largest size (0.419mm-0.841mm) was placed in Reactor 2.3 and filled with water. For this particular size, the maximum flow rate provided by the peristaltic pumps was less than that required from model calculations. Next , the sand of the smallest size was used (0.074-0.21mm). This sand size is about the same as the media that will be used in our reactors. For use in equation 1, the D_{60} was assumed to be 0.15 mm, but this value was not directly measured.

After the arrival of the quartz powde, the upflow velocity test was conducted again to get the actual minimum fluidization velocity and corresponding reactor flow with the media. This was done not only to complete the tests for the sand that is being used in the current reactors, but also because a lack of volume of sand gave very tentative results during the first trial. Two different inlet geometries were used in order to minimize preferential flow, especially at the bottom of the bed. One inlet geometry flowed the water from the bottom of the reactor (figure 4 left), the other flowed the water from both sides near the bottom (figure 4 right).

Confocal Microscopy

Confocal microscopy was used in an effort to better characterize colonization within the anaerobic granules. All images were taken using the Zeiss 710 confocal microscope at The Biotechnology Resource Center Imaging Facility, Cornell

University. A confocal microscope, unlike a standard phase contrast or fluorescent microscope can create images of layers of what is being observed. These images can then be layered, with interpolation between layers, to create a 3 dimensional image of the object. During this semester, images were taken of the granular inoculum fluorescently stained with 4',6-diamidino-2-phenylindole (DAPI), crystal violet, and acridine orange, separately and together. DAPI binds to A-T rich regions of DNA across all domains, crystal violet is used in gram staining to differentiate between gram positive and gram negative bacteria, and acridine orange binds to both DNA and RNA. When bound to DNA, acridine orange has an emission maximum in the green region of light, at 525 nm, and when bound to RNA, the emission maximum shifts to the red region of light, 650 nm.

Results and Analysis

After initial inoculation of reactor 2.1, the first of the AFBR reactors, normal operation only proceeded for one week before the reactor had to be moved and operated in a batch mode for a period of a month. Since then, the reactor has been moved back to it's normal location and returned to standard operating procedure. It has been noted that the gas production within the reactor is far below the level seen while the reactor was in the basement and operated in a semi-batch fashion. Figure 5 shows the intitial gas production rates in Reactor 2.1, and when compared to figure 6, it can be seen gas production has significantly decreased. No data could be collected during batch operation, but there was approximately 150 mL gas produced daily during this time. Though the reactor is now being fed approximately ten times the COD per day as during the batch operation, the gas production is neglible when compared to the previous production levels. Thus, the flow through rate has been lowered to 5 mL/min to achieve a four hour HRT. It is hoped this longer residence time will allow complete degradation of the COD in the reactor and increased gas production. So far, little improvement in gas production rates have occurred, and COD destruction rates have been erratic.

Models

The first model focuses on fluidization and sedimentation velocities, modifying and adding to the model created during the summer. This model relies on the following equations for minimum fluidization velocity and overall density of the support media with adhered biomass:

$$V_{MinFluidization} = \frac{\varepsilon_{FiSand}^3 g D_{60}^2}{36kv(1-\varepsilon_{FiSand})}\left(\frac{\rho_{Sand}}{\rho_{Water}} - 1\right) \tag{1}$$

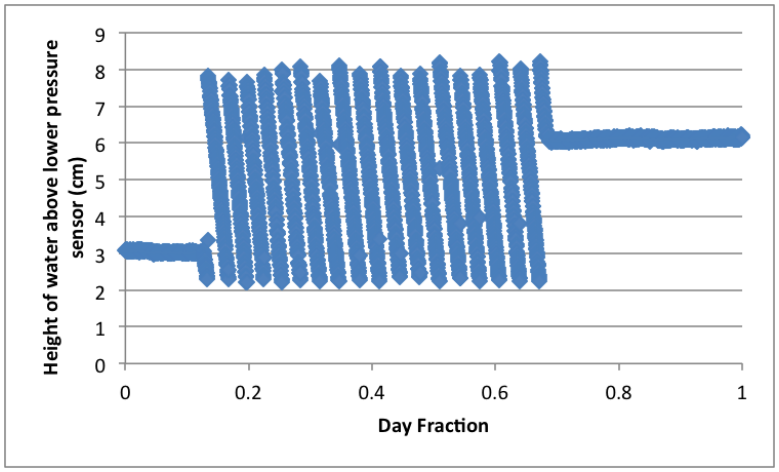

Figure 5: Biogas production in reactor 2.1 on 8/11/13. This production is representative of the gas production during the first week of continuous operation before batch operation. Each vertical line represents on off gas event, releasing approximately 60 mL of gas.

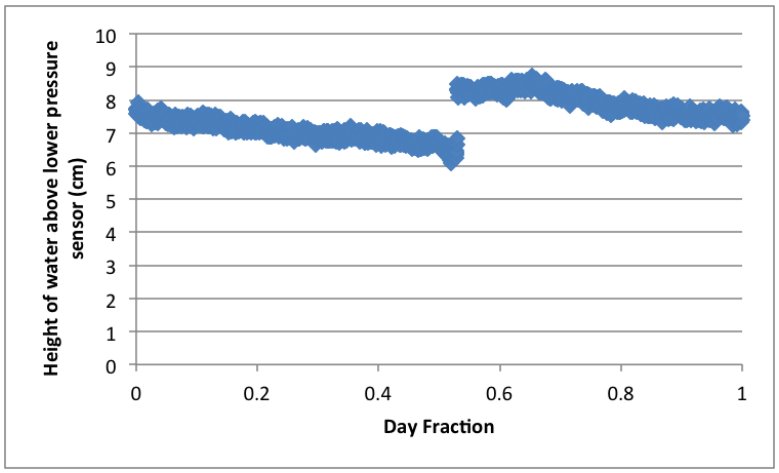

Figure 6: Biogas production in reactor 2.1 on 9/22/13. This production is representative of the low gas levels produced after the reactor was returned to continuous operation after a period of batch operation. According to the graph, approximately 20 mL of gas were produced this day.

Symbol	Variable Name	Symbol	Variable Name
ε_{FiSand}	Porosity of sand bed	υ	Kinematic viscosity of water
g	Acceleration due to gravity	ρ	Density
D_{60}	Diameter which 60% os media is smaller than	r_0	Initial radius of support media
k	Kozeny Constant (assumed equal to 5)	τ	Thickness of Biofilm

Table 4: Variable definitions

$$\rho_{total} = \frac{\rho_{support} r_0^3 + \rho_{bio}\left((r_0+\tau)^3 - r_0^3\right)}{(r_0+\tau)^3} \tag{2}$$

The density of sand in the equation is replaced in this instance with the density of the support material with an attached biofilm as shown in equation 2. Figure 7 shows the beginnings of the model created during the summer and the minimum fluidization velocity of a sand grain with an attached biofilm of varying density. In this model, the sand grain size is 0.5 mm diameter. As can be seen in the model, even relatively small increases in biofilm density cause great increases in the minimum fluidization velocity of particle with an attached biofilm of thickness greater than 0.5 mm.

The first model created this semester similarly shows how the fluidization velocity varies as the biofilm develops for a range of sand sizes. Figure 8 shows the theoretical fluidization velocity according to equation 1 for initial sand grain sizes of 0.1 mm to 1 mm diameter. The graph shows for all grain sizes, the fluidization velocity initially decreases as a biofilm develops before eventually increasing again once the biofilm reaches a certain size, variable with sand grain size. In both Figure 8 and Figure 9, the biofilm is modeled as having a density of 1040 g/L, a value used in the models of Saravanan et al [9]. Both models show a line of constant flow velocity indicating the velocity that must be used to create a 4 hour HRT for the reactors of one meter in height currently used in this study. Though the full scale reactors will likely be far larger than one meter in height, such a small up flow velocity has the capability to fluidize only the smallest sand grains and associated biofilms without recycle. This problem is compounded by a desire to fully expand the bed, not only fluidize it. As shown in Figure 9, 30% bed expansion occurs at roughly double the minimum fluidization velocity. This fact is only based on qualitative data and will be further investigated in the coming weeks.

The models created so far indicate future research will need to focus on the use of other materials besides just sand as a support material and exploration needs to be done into why a minimum HRT of 4 hours is needed for traditional UASBs and AFBRs.

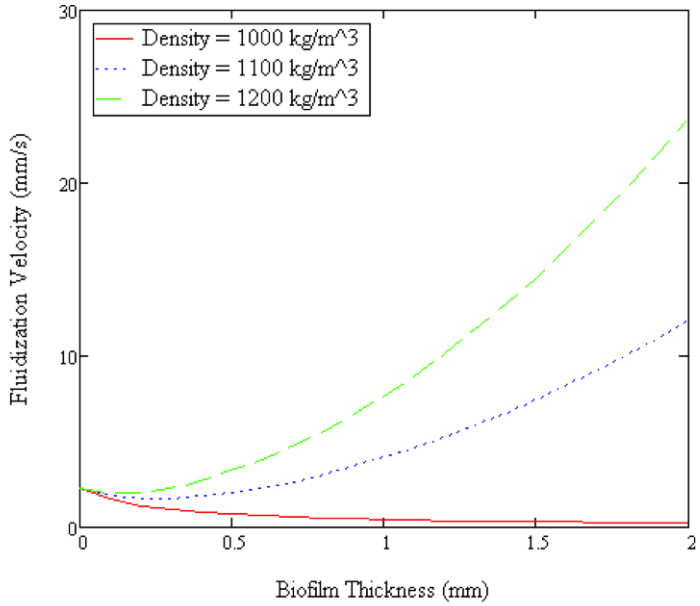

Figure 7: Summer Fluidization Velocity Model with variable biofilm density

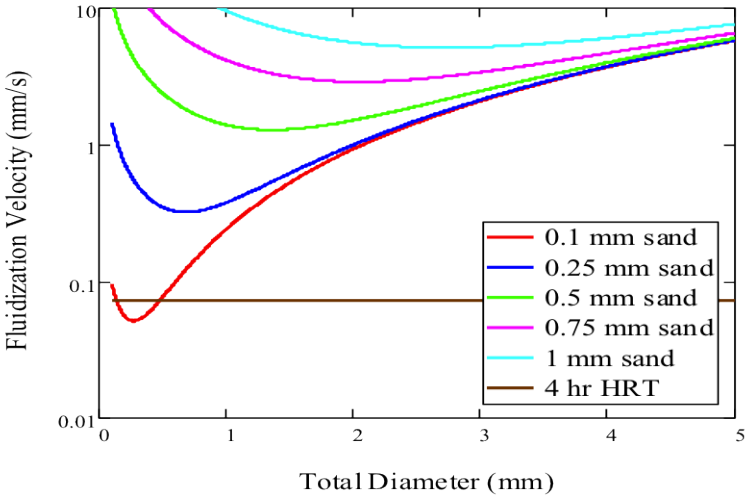

Figure 8: Fluidization velocity during biofilm development for sand of variable size. Biofilm density of 1040 g/L. 4 hour HRT refers to the upflow velocity for a 4 hour HRT in the 1 meter reactors used in this study (0.07 mm/s)

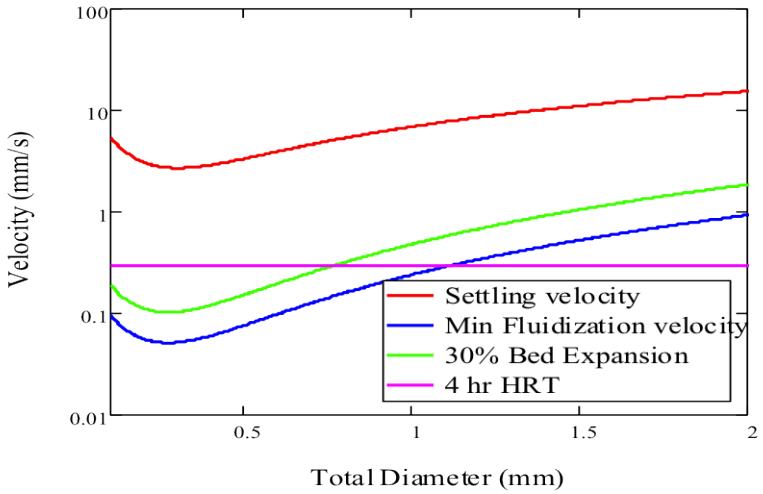

Figure 9: Settling and Fluidization Velocites during biofilm development for 0.1 mm sand. Biofilm density of 1040 g/L.

Bed Expansion

During the first set of experiments, when settled, the sand bed extended a height of 5cm from the bottom of the reactor. Calculations indicate an upflow velocity of 0.215 is required to fluidize the media, however the sand was not fluidized at this flowrate. Upon increasing the flowrate, the media first visually showed signs of fluidization at an upflow velocity of 2.3 mm/s, was deemed fully fluidized at 3.05 mm/s, and started to expand at 3.4 mm/s. The maximum upflow velocity achieved by the pump was 6.1 mm/s and caused a 70% expansion of the sand bed, as shown in figure 10.

In the second set of experiments, when the quartz powder was settled, the bed extended a height of 25cm from the bottom of the reactor, 25 cm above the inlet for geometry 1 and 20 cm above the inlet for geometry 2. Calculations indicate an upflow velocity of 0.096 mm/s is required to fluidize the media, however the quartz powder was not fluidized at the corresponding flow rate of 6.53mL/min on both ways. For the inflow way 1, the media first visually showed signs of fluidization at a flow rate of 20 mL/min.And the expansion of the quartz bed is showed in Figure 11. For the inflow way 2, the media also first visually showed signs of fluidization at a flow rate of 20 mL/min. And the expansion of the quartz bed is shown in Figure 12.

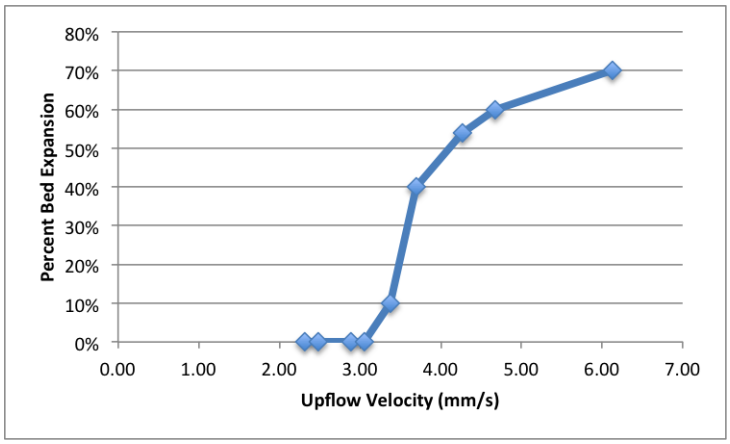

Figure 10: Measured bed expansion at variable upflow velocities. Sand size of 0.07-0.21 mm in diameter with an assumed D_{60} of 0.15 mm.

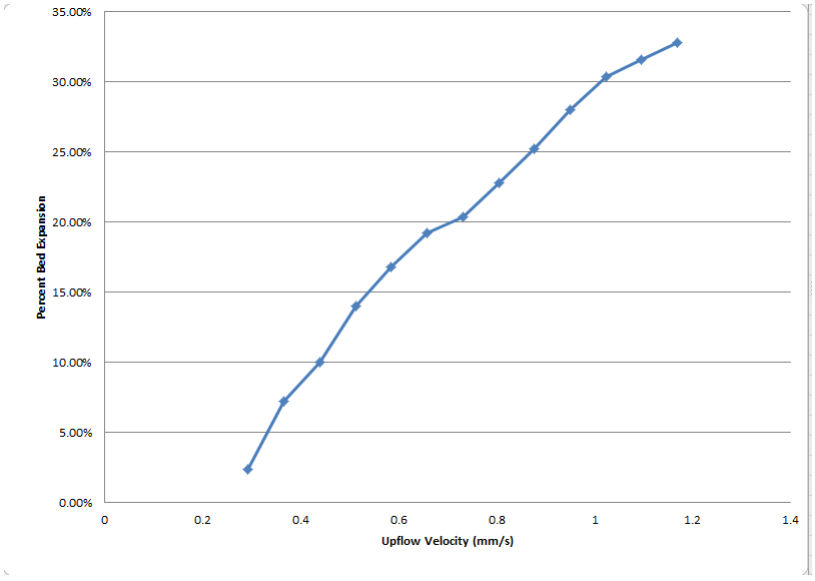

Figure 11: Bed expansion vs. Upflow velocity for inlet geometry 1 and sand of diameter 0.1 mm.

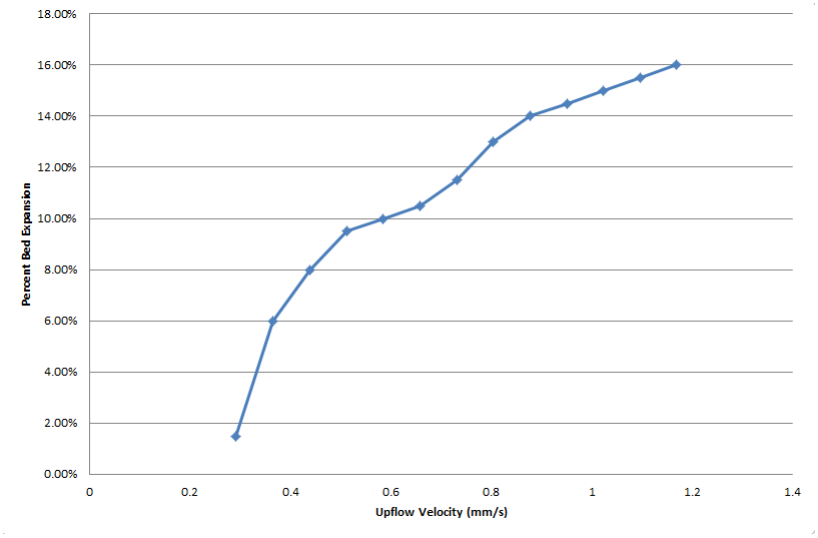

Figure 12: Bed expansion vs. Upflow velocity for inlet geometry 2 and sand of diameter 0.1 mm.

Reactor Performance

COD Removal

The influent is the same for reactors 2.1, 2.2 and 2.3, and the same for reactors 2.4, 2.5 and 2.6. The percent removal of COD for each reactor is calculated for each day. Figures 13 and 14 are a compilation of the Chemcal Oxygen Demand for all six reactors since inoculation.

Biogas Production

UASB reactors 2.4, 2.5, and 2.6 were inoculated on November 22, 2013, hence two weeks of gas production data has been analyzed.The AFBR reactors 2.1, 2.2, and 2.3 comparatively do not have enough data points for sufficient analysis due to a later startup and difficulties in gas capture. Some of the gas capture problem is due to constant agitation of the reactors from the recycle pumps and so the system for gas collection and off gassing is less accurate.

As indicated previously, reactors 2.4, 2.5, and 2.6 receive the same influent.

Reactor 2.4

From the data below , it can be seen that the initial gas production was very low .This is because of initial startup adjustments that occur .Although the graphs for the gas production on each day shows fairly good performance of the reactor

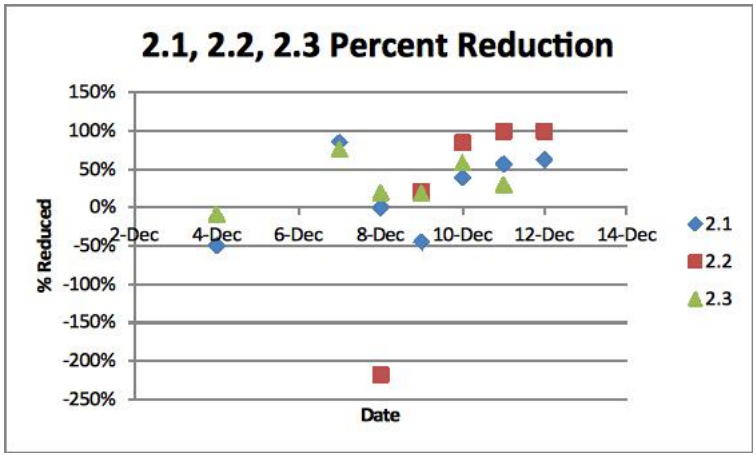

Figure 13: Percent Removal of COD in the AFBR reactors, 2.1-2.3.

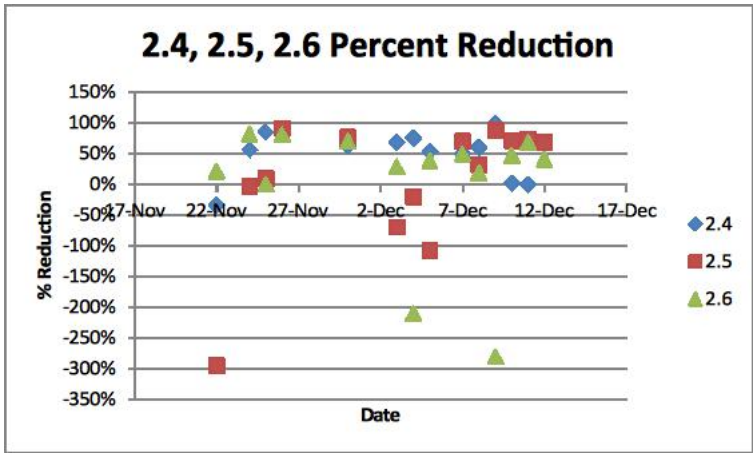

Figure 14: Percent Removal of COD in the UASB reactors, 2.4-2.6

Figure 15: Reactor 2.4 -Volume of Biogas Collected

Reactor 2.4			
Date	Pressure(cm)	Cross sectional area of gas chamber(cm^2)	Volume of biogas collected(cm^3)
11/22/2013	-	11.40	
11/23/2013	4.18		47.63
11/26/2013	4.68		53.33
11/27/2013	16.9		192.58
11/28/2013	11.69		133.21
11/29/2013	5.32		60.62
11/30/2013	20.27		230.98
12/1/2013	2.37		27.01
12/2/2013	20.43		232.80
12/3/2013	25.56		291.26
12/4/2013	29.16		332.28
12/5/2013	38.84		442.59
12/6/2013	42.56		484.98
12/7/2013	15.95		181.75
12/8/2013	21.26		242.26
12/9/2013	13		148.14
12/10/2013	14.75		168.08
Total volume of biogas collected			3269.49

, this amount of data is still insufficient to make a solid conclusion on the trend that the reactor is showing .

The data and graph for reactor 2.4 is as shown in the figures below

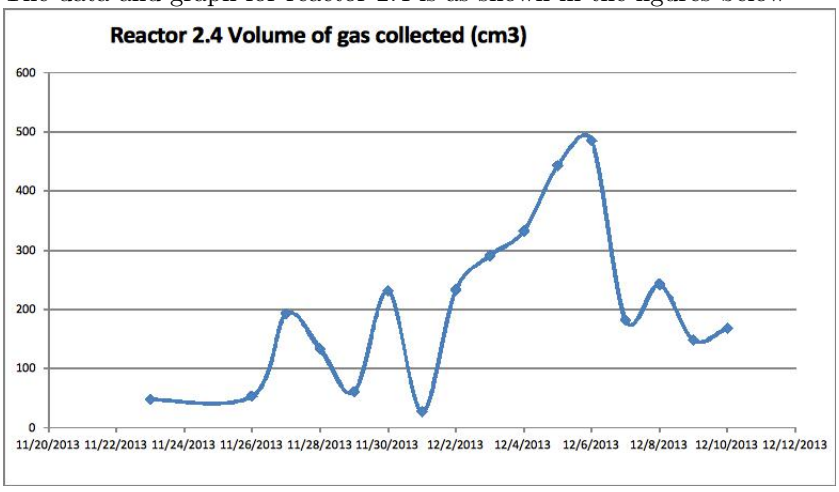

Figure 16 : Reactor 2.4 -Volume of Biogas Collected

Reactor 2.5

Reactor 2.5 has had constant issues with its air tightness and the clogging of the biogranules . In order to unclog the granules, the reactor has been agitated on several occasions which has resulted in sudden release of gas into the gas chamber, but little continuous production of gas has taken place .The data and graphs for this reactor are not yet useful in determining the efficiency of gas production within the reactor.

These two issues need to be fixed to ensure proper working of the reactors . The data then collected will be provide a better insight .

The three graphs below is the pressure data that was graphed on December 6,2013 for reactor 2.4 ,2.5 and 2.6. The graphs for reactor 2.4 and 2.6 show good performance of the reactors while the graph by reactor 2.5 does not provide much information on its performance

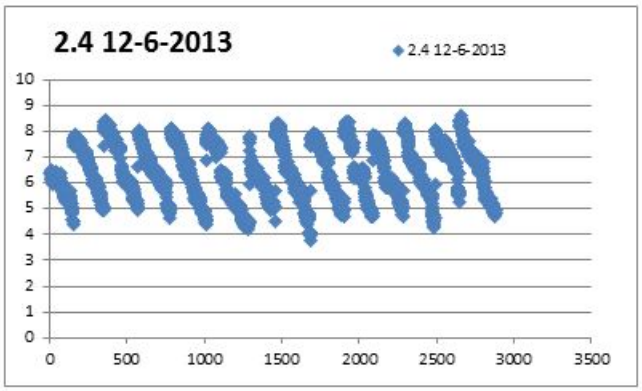

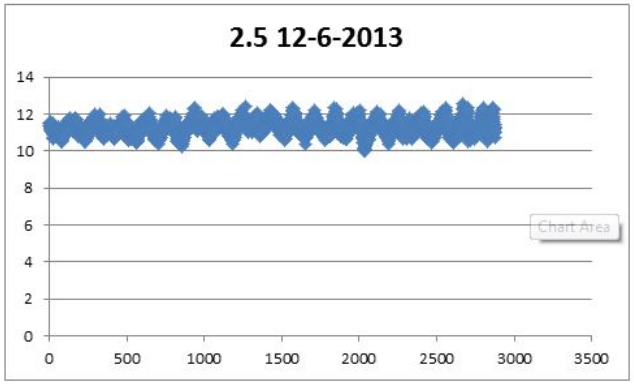

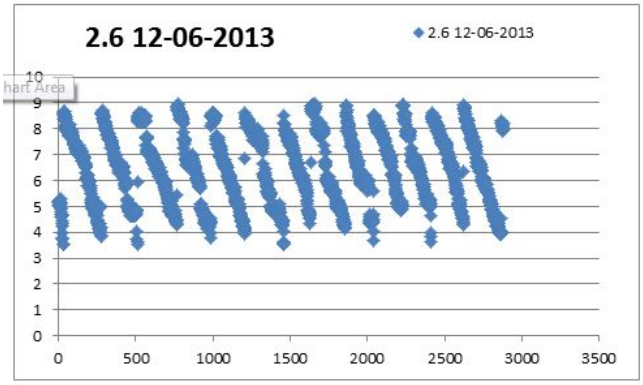

Reactor 2.6

The data and graph for reactor 2.6 is as shown in the figures below

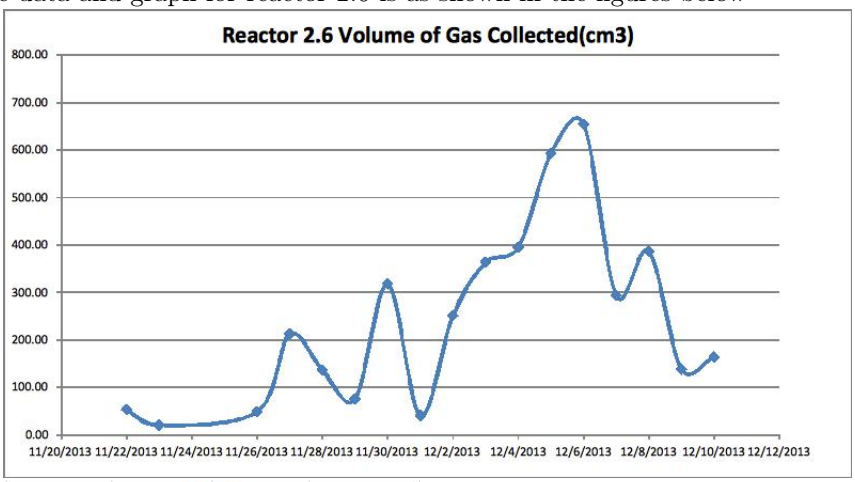

Reactor 2.6			
Date	Pressure(cm)	cross sectional area of gas chamber(cm^2)	Volume of gas collected(cm^3)
11/22/2013	4.63		52.76
11/23/2013	1.82		20.74
11/26/2013	4.32		49.23
11/27/2013	18.69		212.98
11/28/2013	12		136.74
11/29/2013	6.67		76.01
11/30/2013	27.92		318.15
12/1/2013	3.58		40.79
12/2/2013	22.05	11.3951385	251.26
12/3/2013	31.93		363.85
12/4/2013	34.7		395.41
12/5/2013	52.04		593.00
12/6/2013	57.41		654.19
12/7/2013	25.77		293.65
12/8/2013	33.91		386.41
12/9/2013	12.11		138.00
12/10/2013	14.42		164.32
Total volume of biogas collected			4147.49

The graphs for reactor 2.4 and 2.6 show a similar trend which is a very interesting result . The probable cause of this could be that they share a common influent line . This result will be further investigated upon collection of more data .

Though reactor 2.6 has produced more biogas comparatively, a more clear conclusion can be reached once a lot of data is available as to why the trends in biogas production are so similar between reactors 2.4 and 2.6.

Methane Production

Production of methane was able to be monitored through gas chromatography sampling. First a standard curve was deduced for methane within the GC. This curve was deduced by injecting gases with controlled amounts of methane into

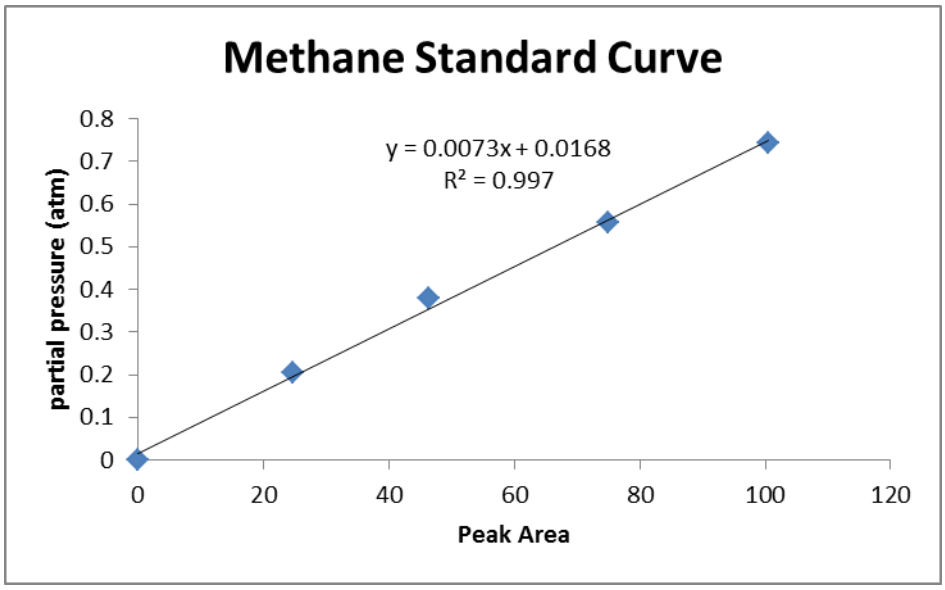

Figure 16: Methane Standard Curve relating peak area data from the GC with true partial pressure of methane

the GC and plotting the peak area values with the partial pressure. With a decent level of certainty, peak area data for methane which is outputted by the GC is directly proportional to the actual partial pressure of the methane delivered. 16 shows the graphical data from the standard curve calculations as well as the resulting linear trend line equation. This curve will be used to equate experimental data points from the reactors with partial pressures of methane.

AFBR reactors 2.1, 2.2, and 2.3 do not have enough data points for methane production as of the date of this publication.

UASB reactors 2.4, 2.5, and 2.6 have had biogas samples taken daily since their inoculation on November 22, 2013. 17 show the partial pressures of methane in the samples gathered over a period of two weeks. Reactors 2.4 and 2.6 show the highest initial partial pressures of methane in the first few days since inoculation, and reactor 2.5 has low initial methane production. This may reflect the fact that reactor 2.5 has had chronic issues with the air-tightness of its gas collection chamber. Complications with the lack of a tight seal on the gas collection area may have a compromising effect on the methane. Reactors 2.4 and 2.6 also show a slight negative trend in methane production, but there are insufficient data points to draw any conclusions from these trends.

It is also suspected that variations in day-to-day results from the GC may be as a result of differing methods of gas extraction and delivery to the GC unit. Investigations in proper methods of sample taking to ensure accurate and consistent results will need to be taken.

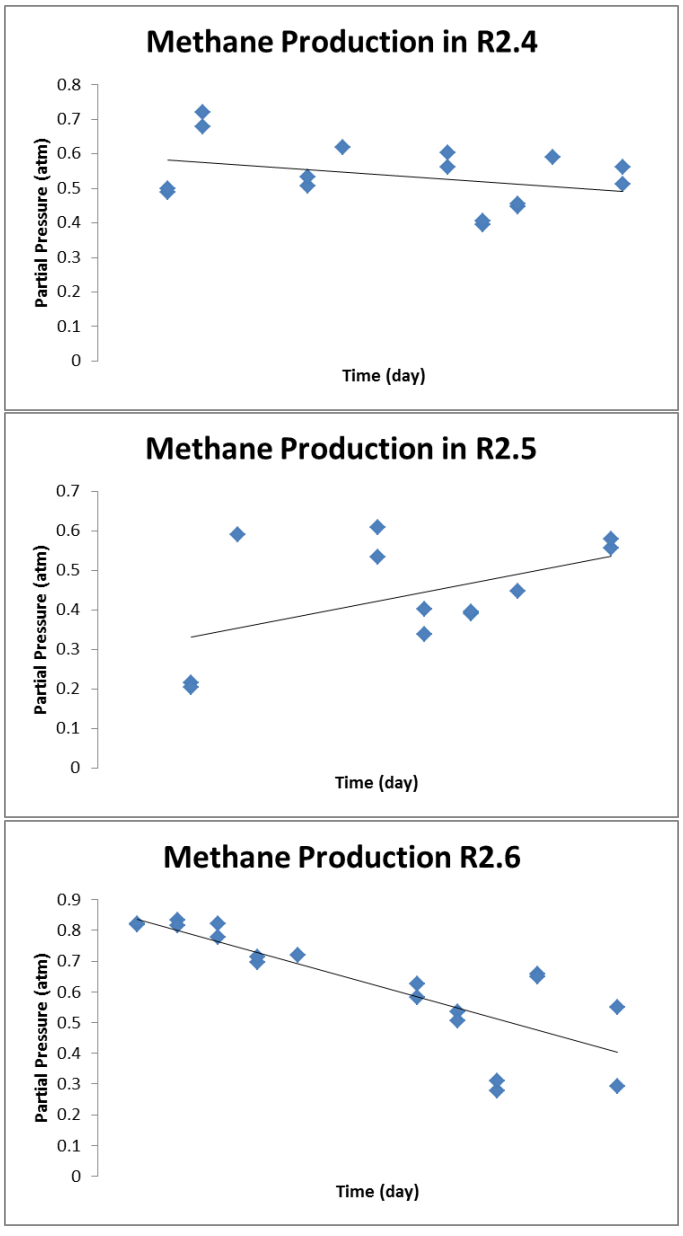

Figure 17: Partial pressures of methane from the UASB reactors 2.4, 2.5, and 2.6

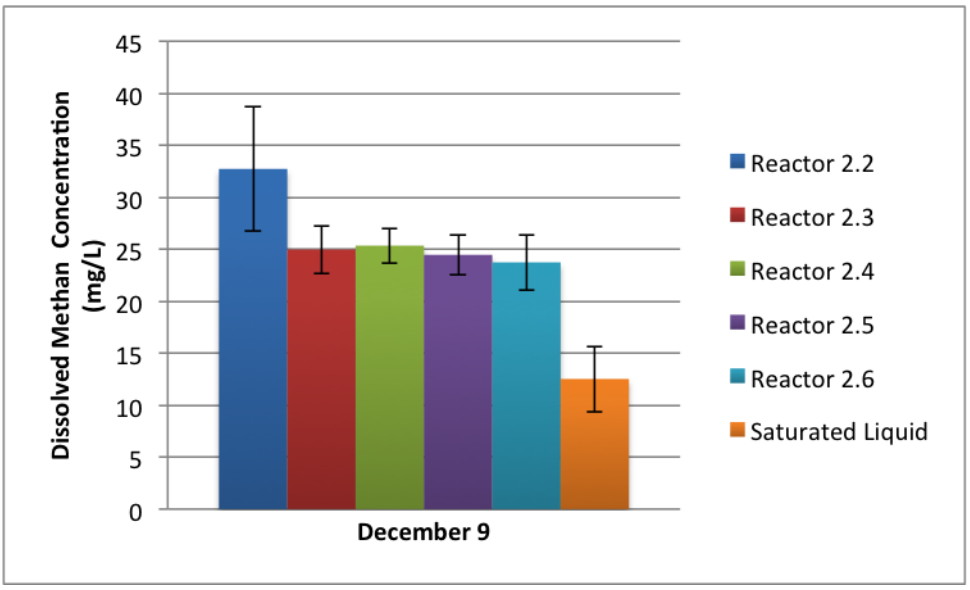

Figure 18: Dissolved methane levels for each reactor and water in equilibrium with the methane in the headspace of the reactors. The data for December 9 was used to represent all days, as two-week data has shown little change in dissolved methane levels in all reactors.

Dissolved Methane

Four dissolved methane measurements were performed on all reactors, 2.2 to 2.6, as reactor 2.1 does not yet have a sampling port for liquid samples before the effluent line. A representative dissolved methane concentration is shown for each reactor in figure 18, with 4 samples for each reactor. As the figure shows, the dissolved methane in each reactor is greater than twice the concentration of saturated water at equilibrium with the gaseous methane captured in the gas chambers. This saturated concentration was calculated by averaging the methane partial pressures in each of the five reactors for December 9.

Granule Characterization

Figures 19 and 20 show a series of images of a granule stained with DAPI. The image area was 50 um x 50 um and is made up of 48 images, each separated by a depth of approximately 0.69 um. As can be seen in both figures the intensity of fluorescence decreases with increased depth into the granule, due to a combination of lack of penetration of the laser and lack of diffusion and binding of the stain at greater depths. This makes it very difficult to create accurate images of the granule makeup beyond the surface. In the future, this problem will be addressed through exploration of cutting the granules and observing the

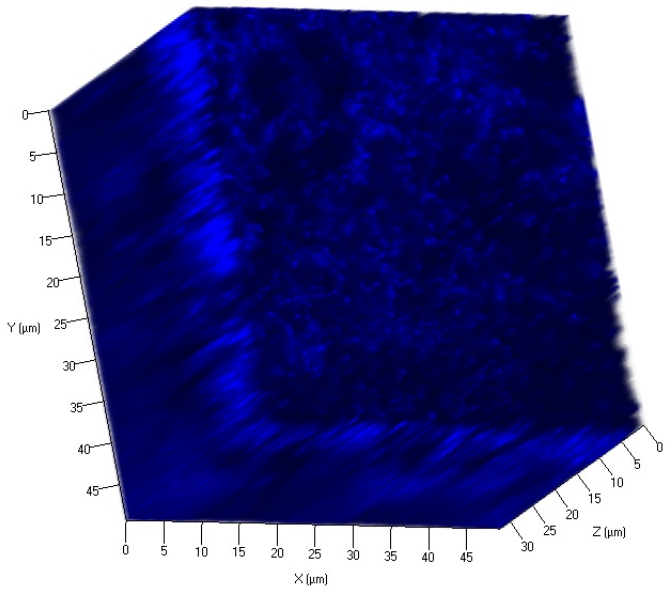

Figure 19: 3D image composed of 48 layers of the granule subsurface constructed through interpolation. The granule was stained with DAPI.

flat section of the granule in order to view its entire depth. The granules are however quite aqueous in nature and cannot withstand much force, so great care must be taken in cutting them. Proposed methods for doing so are suspending the granules in glycerol and freezing them in order to cut them or suspending the granules in agar in order to more easily cut them.

To differentiate between methanogens and bacterial populations, differential staining of DAPI and crystal violet was initially used. However, there is little reason why crystal violet would differentially stain Archaea and Bacteria, so this strategy was abandoned. Instead, characterization was attempted using the discovery that some methanogens have a coenzyme capable of autofluorescence, F420, named for the wavelength at which emission is the greatest [20]. In figure 21, an image of a granule stained with acradine orange, the blue image at the top left shows emission at 420 nm and thus tentatively indicates the presence and location of methanogenic populations. The top right, green image, is light captured at 525 nm, and indicates RNA, whereas the bottom left, red image, is light captured at 650 nm, indicating DNA. Though more information is needed to substantiate the claim, the RNA dense regions may indicate more active microbial populations. The bottom right part of figure 21 is simply an overlay of the other three images in the figure. The strategies used to differentiate microbial populations with acradine orange and autofluorescence will be verified in the future and likely used to further characterize the granule structure.

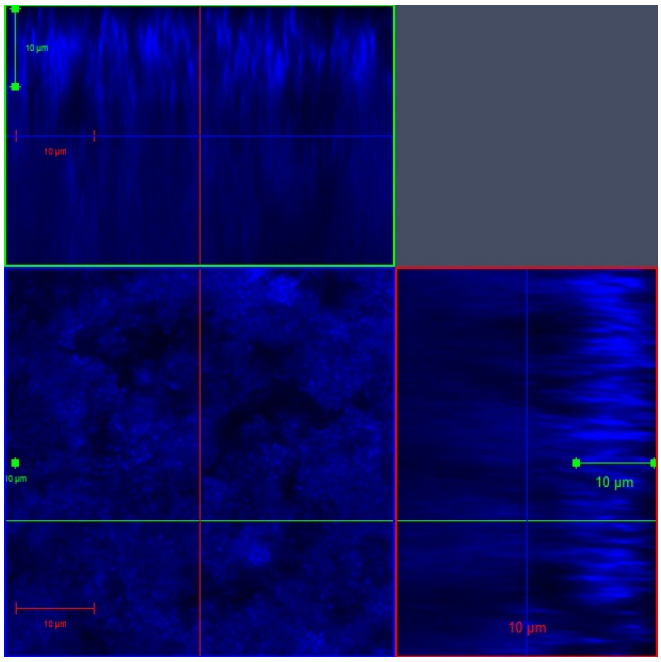

Figure 20: Surface and depth images of the subsurface of a granule, indicating a decrease in fluorescence with increased depth into the granule. The granule was stained with DAPI.

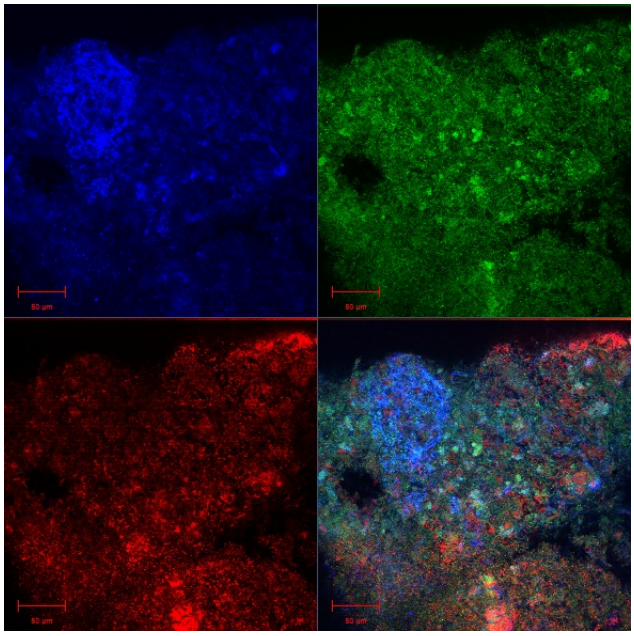

Figure 21: Anaerobic granule stained with acridine orange. Top left shows emission at 420 nm due to autofluorescence of methangens. Top right shows emission by acradine orange at 525 nm, indicating the dye is bound to RNA. Bottom left is emission at 650 nm, indicating the dye is bound to DNA. Bottom right is an overlay of the other images.

Table 5: Physical Properties of Quartz Powder

Property	Value
Diameter (mm)	0.1-0.25
Density (g/m3)	2.65
Bulk Density (g/m3)	1.20

Kremer Pigmente, quartz powder supplier

Conclusions

A number of conclusions can be derived from the particle fluidization and settling model on the behavior of particles in the fluidized bed reactor. Both fluidization velocity and settling velocity of a bed of support media are related to the size of density of the support media particles. Both velocities increase as diameter and density increase. Particles with an initial diameter of 0.1mm, a low value for a typical sand particle diameter, require the lowest fluidization velocity to properly fluidize, and the lowest settling velocity to settle. Since we desire our reactors to have a relatively high hydraulic residence time, we will use support media with the desired small size. Quartz powder, a finer grade of silica sand, has a small enough particle diameter and density to support our desired flow regime. Table 5 lists some of the physical properties of quartz powder.

Additionally, knowledge of the behavior of smaller sized particles in the reactor will help the team alleviate the need for a recycle to achieve an ideal upflow velocity for particle fluidization.

Future Work

Model Development

A model still needs to be developed to determine the relationship between the flow in the reactor and granule size and robustness. The model will likely be an adaptation of a previous model relating the specific energy dissipation rate within a fluidized bed to bioparticle size and distribution [21].

The last model, a sort of biokinetic model, will deal more directly with the microbial communities present in the reactor with the overall goal of determining what limits the rate of COD destruction in the reactor. It is assumed now that mass transfer from the bulk fluid to the surface of the biofilm or surface of the granules is the rate limiting step within the reactor. The model will elucidate at what rate the substrate enters the microbial community and may serve to identify a relationship between the organic loading rate of the reactor and the necessary surface area of microbes to effectively degrade the substrate. Further model development will model the growth of different microbial species

in the reactor as well as concentrations of the substrates for these communities, ie complex carbohydrates, simple carbohydrates, acetate, and methane as a product.

Reactor Operation

Before the Spring of 2014, it is planned to move the reactors to a temperature controlled room, where it will be easier to keep the reactors at an elevated temperature. This elevated temperature will likely improve the performance of the anaerobes within the reactors and will more accurately represent the climatic conditions where the reactors will eventually be in use.

A recurring problem, primarily for the AFBRs, has been the design of an effective inlet system. To properly fluidize the bed, flow must be uniform upon entering the reactor. In the stacked rapid sand filter, this is acheived through cutting slits in a horizontal pipe, but this will not work for sand as fine as is used in the AFBRs. The sand this fine is also extremely prone to clogging the reactors. Though an operational reactor can remain in operation indefinitely without clogging, the reactors do periodically need to be turned off, and this is when the clogging occurs. Both an influent design as well as an operation strategy need to be determined to prevent clogging and create fully fluidized flow.

In both types of reactor, the biogranules need to be made more robust. Breakup of granules in the UASBs needs to be prevented. During each operation, after a period of roughly two weeks to a month, the granules begin to become fluffy and more prone to stick together and wash out. Research need to be conducted to discover if this is due to characteristics of the influent, and if so, if there is another way to keep the granules from breaking up. Influent characteristics will be extremely vairable during implementation, and so altering the wastewater composition is likely not an option to improve control ofthe granules. In the AFBRs, during long term operation, there should be very little biomass in the reactors that is not adhered to the support media. Thus, a method needs to be created to improve adherence of biomass to the support media and then to washout all biomass not adhered to media. After this start up period, steady state operation improvements can be made.

As indicated by the dissolved methane measurements in all reactors, the liquid effluent is supersaturated with methane. Future research will identify ways in which methane transfer from liquid to gas phase can be improved for greater methane capture and eventual use. A mixing mechanism of some sort would likely improve mass transfer, though this would also suggest greater mass transfer should already be occuring in the AFBRs. Measurements so far would indicate this is not the case, so other ideas and designs must be developed.

Trip to Honduras

The members of the wastewater team will be traveling two Honduras for two weeks in early January to learn about the culture of waste and wastewater

there. A report will be constructed upon return from the trip in order to better motivate research into wastewater treatment. Though the research in this study will not be used abroad in the short term, it will remain important to design reactors for real world use.

References

[1] Burton, Franklin, Harold Leverenz, Ryujiro Tsuchihashi, and George Tchobanoglous. "Water reuse: issues, technologies, and applications." (2007): 392.

[2] McCarty, Perry L., Jaeho Bae, and Jeonghwan Kim. "Domestic wastewater treatment as a net energy producer–Can this be achieved?." Environmental science & technology 45.17 (2011): 7100-7106.

[3] Kim, Jeonghwan, Kihyun Kim, Hyoungyoung Ye, Eunyoung Lee, Chungheon Shin, Perry L. McCarty, and Jaeho Bae. "Anaerobic fluidized bed membrane bioreactor for wastewater treatment." Environmental science & technology 45, no. 2 (2010): 576-581.

[4] S. Aiyuk, I. Forrez, D. K. Lieven, A. van Haandel, and W. Verstraete, "Anaerobic and complementary treatment of domestic sewage in regions with hot climates–a review," Bioresour. Technol., vol. 97, no. 17, pp. 2225–2241, Nov. 2006.

[5] M. M. Ghangrekar, S. R. Asolekar, and S. G. Joshi, "Characteristics of sludge developed under different loading conditions during UASB reactor startup and granulation," Water Research, vol. 39, no. 6, pp. 1123–1133, Mar. 2005.

[6] S. Chong, T. K. Sen, A. Kayaalp, and H. M. Ang, "The performance enhancements of upflow anaerobic sludge blanket (UASB) reactors for domestic sludge treatment–a state-of-the-art review," Water Res., vol. 46, no. 11, pp. 3434–3470, Jul. 2012.

[7] L. C. S. Lobato, C. A. L. Chernicharo, and C. L. Souza, "Estimates of methane loss and energy recovery potential in anaerobic reactors treating domestic wastewater," Water Sci. Technol., vol. 66, no. 12, pp. 2745–2753, 2012.

[8] Lettinga, G., and LW Hulshoff Pol. "UASB-process design for various types of wastewaters." Water Science & Technology 24, no. 8 (1991): 87-107.

[9] Saravanan, V., and T. R. Sreekrishnan. "Modelling anaerobic biofilm reactors—A review." Journal of Environmental Management 81.1 (2006): 1-18.

[10] Iza, J. "Fluidized bed reactors for anaerobic wastewater treatment." Water Science & Technology 24.8 (1991): 109-132.

[11] Elmitwalli, Tarek, et al. "Anaerobic biodegradability and treatment of Egyptian domestic sewage." Journal of Environmental Science and Health, Part A 38.10 (2003): 2043-2055.

[12] "Water Vs. Wastewater." Water Vs. Wastewater. Huntsville Water Pollution Control, 2001. <http://www.huntsvillewpc.org/oldsite/differences.htm>.

[13]"The Biogas." Biogas Composition. Naskeo Environnement, 2009. <http://www.biogas-renewable-energy.info/biogas_composition.html>

[14] "Wastewater and Public Health." On-Site Wastewater Disposal and Public Health. Purdue University, n.d. <https://engineering.purdue.edu/~frankenb/NU-prowd/disease.htm>. From Pipeline, Summer 1996, Vol.7, No.3

[15] Lono-Batura, Maile, Yinan Qi, and Ned Beecher. "Biogas Production And Potential From U.S. Wastewater Treatment." <http://www.biocycle.net/2012/12/18/biogas-production-and-potential-from-u-s-wastewater-treatment/> BioCycle. N.p., Dec. 2012. Vol. 53, No. 12, p. 46

[16] United Nations. United Nations Education, Scientific and Cultural Organization. *World Water Development Report*. 2003.

[17] S. Aiyuk and W. Verstraete, "Sedimentological evolution in an UASB treating SYNTHES, a new representative synthetic sewage, at low loading rates," Bioresour. Technol., vol. 93, no. 3, pp. 269–278, Jul. 2004.

[18] J.-S. Huang and C.-S. Wu, "Specific energy dissipation rate for fluidized-bed bioreactors," Biotechnology and Bioengineering, vol. 50, no. 6, pp. 643–654, 1996.

[19] Lide and Frederikse. CRC Handbook of Chemistry and Physics, 76th Edition, D. R. Lide and H. P. R. Frederikse, ed(s)., CRC Press, Inc., Boca Raton, FL, 1995.

[20] H. J. Doddema and G. D. Vogels, "Improved identification of methanogenic bacteria by fluorescence microscopy.," Appl. Environ. Microbiol., vol. 36, no. 5, pp. 752–754, Nov. 1978.

[21] J.-S. Huang and C.-S. Wu, "Specific energy dissipation rate for fluidized-bed bioreactors," Biotechnology and Bioengineering, vol. 50, no. 6, pp. 643–654, 1996.